



# Experimental Study on Acoustic Emission and Ultrasonic Testing Technology with Fiber Bragg Gratings Sensing

Lijun Meng<sup>1</sup>(✉), Han Zhang<sup>1</sup>, Qianpeng Han<sup>1</sup>, and Junjie Huo<sup>2</sup>

<sup>1</sup> College of Intelligent Manufacturing, Jiangnan University,  
No. 8 San Jiao Hu, Caidian District, Wuhan, China  
menglijun0408@163.com

<sup>2</sup> Wuhan City Vocational College, No. 127 Nan Li, Hongshan District, Wuhan, China

**Abstract.** The combination of fiber Bragg gratings (FBG) sensing with acoustic emission and ultrasonic detection can make full use of the advantages of various technologies to realize the comprehensive damage detection of equipment in harsh environment. Firstly, the acoustic emission signals of the gas tank under different impact heights caused by steel ball were detected by FBGs, and the signals were analyzed by using Fourier transform and Hilbert-Huang transform method. The results showed that the acoustic emission intensity measured by FBG increases with the impact height and internal pressure; the main frequencies of Hilbert Huang transform spectrum were not obviously affected by the impact height; while the main frequency band of Hilbert Huang signals was increased after inflation. Then, this FBG was used to detect the ultrasonic wave propagating in the gas tank before and after the artificial defect. The results reflect that the main frequencies before and after the defect was basically the same, but the signal amplitude decreased and the main frequency wave packet dispersed and lagged a lot when there was a defect. It provides experimental basis and effective signal processing method for the simultaneous measurement of acoustic emission and ultrasonic detection with FBG.

**Keywords:** FBG · Acoustic emission · Ultrasonic detection · Hilbert-Huang transform

## 1 Introduction

Large equipment with advanced technology and complex structure, such as water turbine generator, pressure vessel, and aeroengine, plays an extremely important role in the national economic construction. The real-time monitoring and diagnosis of their operating states is of great significance to ensure their safe operation and nonoccurrence of serious accidents. Currently, there are dozens of nondestructive testing methods commonly used, such as leakage testing, magnetic particle testing, ultrasonic testing, acoustic emission testing, and ray testing [1, 2]. However, single testing technology has its own

limitations and often cannot identify all forms of damage. The integration and innovation of various detection technologies is a development direction in the future. Some researchers combine acoustic emission and ultrasonic technology to study the deformation stage in metals, the fracture of friction-stir-welded joints, gas tungsten arc welding quality and so on [3–6]. Acoustic emission technique can be used for internal crack extension of continuous dynamic real-time detection and recognition, and ultrasonic testing technology can be employed to locate static damage and measure damage size by using the reflection, scattering and other signal characteristics of the ultrasonic wave artificially launched or generated inside the specimen, therefore the technology combining these two methods to detect pressure vessel damage can help us to understand the damage state and the damage evolution mechanism more comprehensively [7]. However, the current acoustic emission and ultrasonic composite detection technology mainly uses piezoelectric ceramics to detect acoustic signals, and it has disadvantages such as large volume, easy to be affected by electromagnetic interference, etc. Fiber Bragg grating (FBG) sensors have become the preferred component instead of piezoelectric ceramics due to their high sensitivity, strong anti-interference ability, good insulation, compact structure and easy construction of sensor network [8]. The current researches mainly focus on detecting Lamb waves or artificial acoustic emission sources in thin plates [9–11], and there are few studies on actual equipment structures.

Based on FBG sensing, it is studied the acoustic emission produced by steel ball impact and ultrasonic waves before and after man-made damage in the gas tank, and the signals detected by FBG is analyzed with Fourier transform and Hilbert-Huang transform method.

## 2 Acoustic Emission Detection Experiment

The experimental principle is shown in Fig. 1. The FBG was glued on the surface of the gas tank with epoxy resin adhesive, and the acoustic emission signal was generated by the steel ball free-fall impact from high to the fixed position of the gas tank. FBG was arranged along the acoustic propagation path to measure the acoustic emission signal. The wavelength demodulation system based on a tunable laser was established. The light emitted by the tunable laser reached the FBG through the coupler, and then the photodetector received the reflected light and converted the light intensity change into electrical signal which was displayed by the oscilloscope. In the experiment, a steel ball with a diameter of 6 mm was used, the length of the fiber grating was 3 mm, and the distance from the impact point to the fiber grating center was 100 mm. The adjustable laser was Yenista-T TLS-AG-C, and Thorlabs-PDA-10CS was chosen as photodetector; digital oscilloscope was Tektronix TBS-1102.

Experiments were carried to detect the acoustic emission under different steel ball impact heights with FBG, when there is no gas or a certain high-pressure gas in the gas storage tank. Figure 2 showed the FBG signal when there was no gas in the storage tank and the impact height was 700 mm. Its main frequency in Fourier transform result was around 195.3 kHz. The impact acoustic emission is the superposition of guided wave with multiple modes. It is difficult to analyze the impact acoustic emission only by time domain or simple frequency domain analysis owing to waveform transformations and

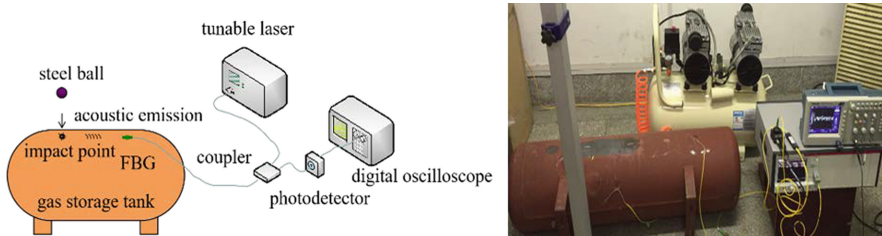


**Fig. 1.** Schematic diagram of steel ball impact acoustic emission experiment

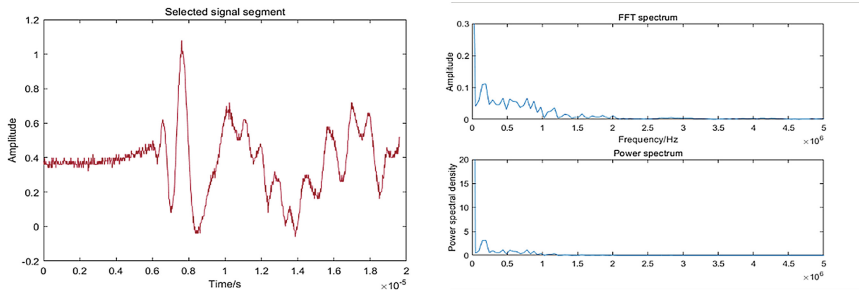


**Fig. 2.** Acoustic emission signal and its Fourier transform result of no-load gas tank with 700 mm impact height

signal attenuation in the propagation process. Therefore, Hilbert-Huang transform was used to study the impact acoustic emission.

Figure 3 showed the empirical modal analysis results of the signal in Fig. 2. In Fig. 3, the signal was decomposed into imf1-imf7 modal function and residual component res. Removing low intensity components and noise, it mainly analyzes the modal components of imf3-imf6 in this paper. The instantaneous envelope and instantaneous frequency curves of the imf3-imf6 component were mainly concentrated around 800 kHz, 600 kHz, 400 kHz, and 120 kHz.

In order to better reflect the signal frequency change with time, the Hilbert-Huang spectrum line was obtained in Fig. 4. From Fig. 4, the acoustic emission was composed of many mode waves with different frequencies. During the initial phase, each frequency band energy was relatively low; as time goes by, the high-frequency energy increased rapidly and gradually converted to a relatively low high-frequency signal. After the peak-to-peak point of the acoustic emission signal (after 8  $\mu$ s in Fig. 4), the high-frequency signal fluctuated in different mode waves, and the energy gradually decreased. Finally, with the further loss of energy, it oscillated greatly in all frequency range. The center frequency of the 120 kHz–50 kHz band signal existed throughout the whole period. The guided wave energy of each frequency was continuously converted over time. Therefore, the peak-to-peak value in time domain was used to reflect the impact intensity, and the Hilbert-Huang spectrum was used to analyze the guided wave mode change.

First, the response of FBG to the acoustic emission propagating on gas tank surface with no compressed gas was studied. During the experiment, steel balls were freely

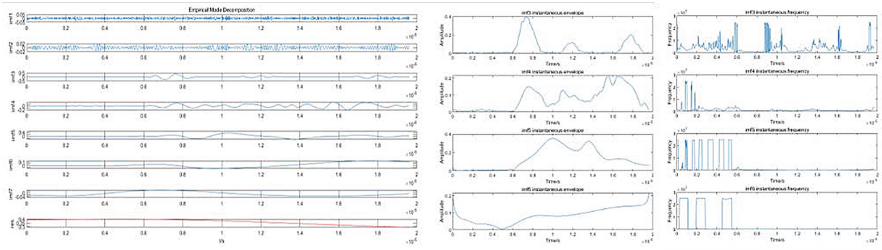


**Fig. 3.** Empirical mode decomposition results

falling from different heights to the fixed position of the gas tank. Figure 5 showed the peak-to-peak change of the FBG acoustic emission signal increased with the impact height. Its amplitude characteristic can reflect the intensity change of the surface acoustic emission. Figure 5 also showed the dominant frequency of higher energy and relatively long duration in the Hilbert-Huang spectrum at different impact strengths, and the guided waves dominant frequency remained basically unchanged (mainly 80 kHz–330 kHz) at different impact heights, which was consistent with the constant impact of the same steel ball. These analyses showed that the FBG frequency domain characteristics can be used to identify and detect the acoustic emission source, and the signal amplitude can reflect its impact intensity.

Then, the response of the FBG to the acoustic emission propagating on loaded gas tank of 400 kPa pressure was studied. The steel balls were freely falling from 300 mm to 900 mm to the gas tank surface. The same FBG was used to measure each acoustic emission in turn. Figure 6 showed the changes of signal peak-to-peak value and the main frequency in Hilbert Huang spectrum with the impact height. The peak-to-peak value fluctuated with impact height, and the main frequencies of the Hilbert Huang spectrum were basically stable in the range of 110 kHz–430 kHz, and these main frequencies were increased compared with the no-load ones. This indicates that when there is compressed gas in the gas tank, the guided wave frequencies of the acoustic emission signal measured by the FBG pasted on the surface will be increased.

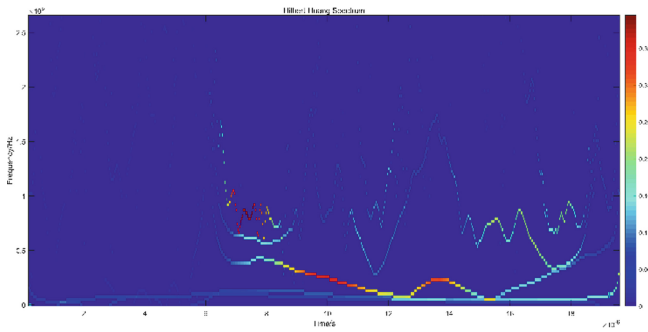


**Fig. 4.** Hilbert-Huang spectrum

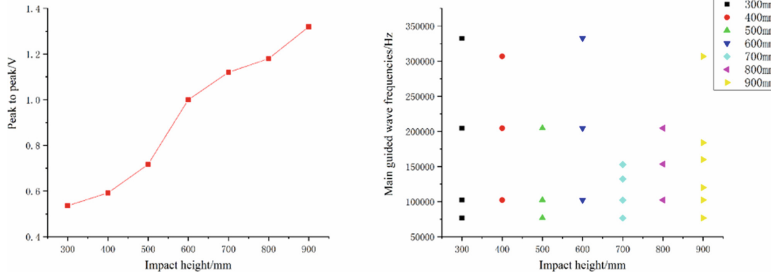


Fig. 5. Analysis results under different impact heights when the gas tank is empty

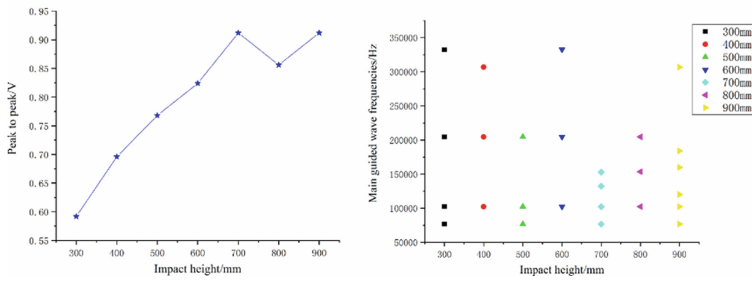


Fig. 6. Analysis results under different impact heights with pressure of 400 kPa

In addition, acoustic emission experiments under different gas pressures pressure were studied. The gas tank was filled with different compressed gas from 100 kPa to 600 kPa pressure, and the steel ball fell at 700 mm. The response signals of the FBG to the impact acoustic emission were recorded in turn. The signal results were shown in Fig. 7. From the figure, the peak-to-peak value increased slightly non-linearly with the internal pressure, while the of the main frequency change with gas pressure was not obvious.

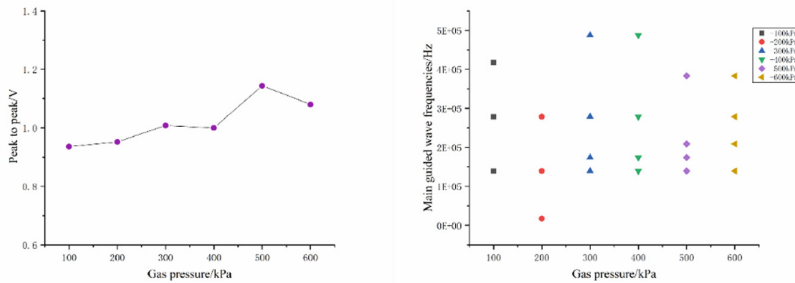
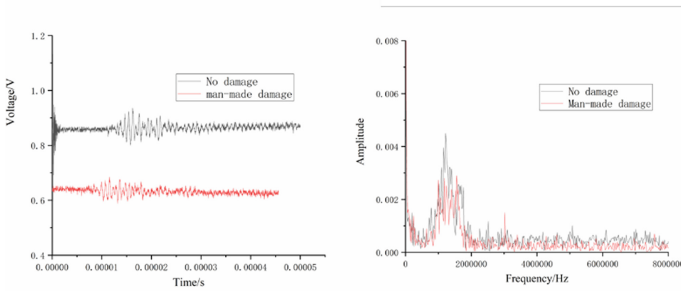


Fig. 7. Analysis results under different gas pressures with 700 mm impact height

### 3 Detection of Artificial Damage on the Surface of Gas Tank Under Ultrasonic Excitation

The experimental setup was similar to Fig. 8. The ultrasonic transmitter and receiver card was used to generate high-voltage pulse signals to stimulate the probe to generate ultrasonic wave on the surface of the gas tank. The duration of the high-voltage pulse signal was 1  $\mu\text{s}$ , and the voltage amplitude was 300 V. A double crystal oblique probe of 1.5 MHz was adopted, and the distance between the ultrasonic incident point and the FBG center was 50 mm. First, the FBG was used to measure the ultrasonic wave when there was no damage on the gas tank surface. Then an artificial damage was made by AB glue in the path of ultrasonic propagation. The man-made damage was a slender rectangle 25 mm away from the incident point, and its direction was perpendicular to the ultrasonic axis. Then the FBG was employed to measure the ultrasonic wave again.

The ultrasonic signals measured before and after the man-made defects were shown in Fig. 8. From the Fourier transform and the Hilbert yellow spectrum shown in Fig. 8 and Fig. 9, the ultrasonic wave with the center frequency of 1.2 MHz was detected, which was basically the same as the center frequency of the probe. It can be seen from the main frequencies and response amplitude of Hilbert-Huang spectrum that the main frequencies of the response signal before and after the damage were basically in the range



**Fig. 8.** Time-domain and FFT signal of fiber grating before and after man-made damage

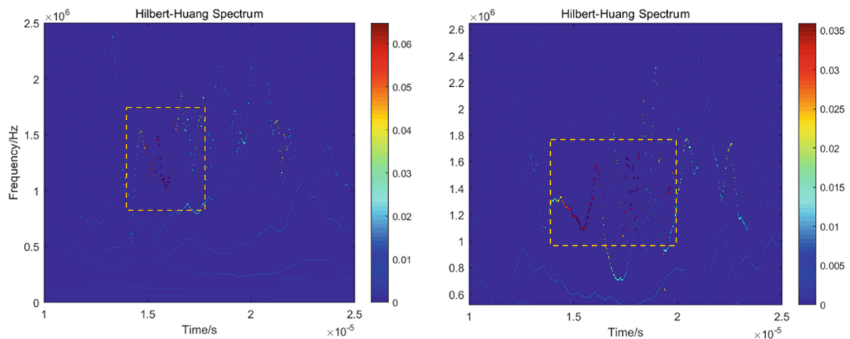


**Fig. 9.** Hilbert-Huang spectrum of FBG before and after man-made damage

of 1–1.5 MHz, while the signal energy showed a significant drop. After the damage, the dominant frequency of the detected signal was more dispersed and lagged. This should be due to the delay caused by ultrasound scattering after encountering man-made damage, bypassing the damage edge and propagating along the acoustic axis. Therefore, the damage can be judged by the signal amplitude change, and the damage position can be further determined by analyzing the delay of the main frequency wave packet.

## 4 Conclusion

The impact acoustic emission and ultrasonic wave detection of gas storage tanks using FBG were studied. The signals were compared and analyzed by the Fourier transform and Hilbert-Huang transform methods. By using free-falling steel ball to hit the outer surface of the gas tank to generate acoustic emission, the effects of impact height of steel ball and charging pressure of gas tank on impact acoustic emission measured by FBG were studied experimentally. It showed that the FBG peak-to-peak value increased with the impact height, and the effect of charging pressure on peak-to-peak value was not obvious; the dominant frequencies of Hilbert spectrum signal were basically not affected by the impact height, while the dominant frequency of the Hilbert spectrum increases as the gas tank is filled. In addition, the same FBG was used to detect the ultrasonic wave on the surface of the gas tank. The dominant frequencies of the ultrasonic guided waves measured by the FBG were basically the same before and after the man-made damage, while the response amplitude decreased significantly and the arrival time of the dominant guided wave has a certain delay when there was damage.

**Acknowledgments.** This study was supported by the Natural Science Fund of Hubei Province in China under grant No. 2019CFB590 and National Natural Science Foundation of China under grant No. 51505187.

## References

1. Kumpati, R., Skarka, W., Ontipuli, S.K.: Current trends in integration of nondestructive testing methods for engineered materials testing. *Sensors* **21**(18), 6175 (2021)
2. Huan, H.T., Liu, L.X., Mandelis, A., Peng, C.L., Chen, X.L., Zhan, J.S.: Mechanical strength evaluation of elastic materials by multiphysical nondestructive methods: a review. *Appl. Sci.-Basel* **10**(5), 1588 (2020)
3. Vetrone, J., Obregon, J.E., Indacochea, E.J., Ozevin, D.: The characterization of deformation stage of metals using acoustic emission combined with nonlinear ultrasonics. *Measurement* **178**, 109407 (2021)
4. Stepanova, K.A., Kinzhagulov, I.Y., Yakovlev, Y.O., Kovalevich, A.S., Ashikhin, D.S., Alifanova, I.E.: Applying laser-ultrasonic and acoustic-emission methods to nondestructive testing at different stages of deformation formation in friction stir welding. *Russ. J. Nondestruct.* **56**(3), 191–200 (2020)
5. Zhang, L., Basantes-Defaz, A.C., Ozevin, D., Indacochea, E.: Real-time monitoring of welding process using air-coupled ultrasonics and acoustic emission. *Int. J. Adv. Manuf. Technol.* **101**(5–8), 1623–1634 (2019)

6. Thiagarajan, J.S.: Non-destructive testing mechanism for pre-stressed steel wire using acoustic emission monitoring. *Materials* **13**(21), 5029 (2020)
7. Li, H.R., Dong, Z.K., Ouyang, Z.L., Liu, B., Yuan, W., Yin, H.W.: Experimental investigation on the deformability, ultrasonic wave propagation, and acoustic emission of rock salt under triaxial compression. *Appl. Sci.-Basel* **9**(4), 635 (2019)
8. Wu, Q., Okabe, Y., Yu, F.: Ultrasonic structural health monitoring using fiber Bragg grating. *Sensors* **10**, 3395 (2018)
9. Yu, F., Okabe, Y.: Linear damage localization in CFRP laminates using one single fiber-optic Bragg grating acoustic emission sensor. *Compos. Struct.* **238**, 1119929 (2020)
10. Tsuda, H., Lee, J.-R., Guan, Y., et al.: Investigation of fatigue crack in stainless steel using a mobile fiber Bragg grating ultrasonic sensor. *Opt. Fiber Technol.* **03**, 209–214 (2007)
11. Zhu, Y.K., Chong, B., Lin, X.M.: Acoustic emission localization method for damage of composite material sheet based on intensity-type optical fiber sensing technology. *Non-destruct. Monit.* **33**, 56–60 (2011)